Bulletin of Volcanology (2026) 88:18
https://doi.org/10.1007/s00445-026-01941-5

SHORT SCIENTIFIC COMMUNICATION

The volume of explosive products erupted during the ~ 1700 CE eruption of *Sii Aks* (Tseax), Canada

Sara Osman[1] · Thomas J. Jones[1] · Kelly N. McCartney[1] · Yannick Le Moigne[2,4] · James K. Russell[3] · Glyn Williams-Jones[4]

Received: 14 September 2025 / Accepted: 11 January 2026

Abstract
Small mafic explosive eruptions are a globally common and frequent eruption type, and understanding the size of past eruptions is key to preparing for future impacts. However, Canadian volcanoes have received relatively little investigation due in part to their location in remote and challenging terrain. Here, we measured tephra thicknesses from 96 locations for the ~ 1700 CE eruption of *Sii Aks* (Tseax) in the Northern Cordillera Volcanic Province, British Columbia, a region of active volcanism and rifting in northwest Canada. We used these data to produce isopach maps and estimate the volume of tephra fall during the eruption, using exponential, power law, and Weibull functions. We find the values are consistent across the different methods at $2.5 - 3.4 \times 10^6$ m^3, thus classifying the eruption as two on the Volcanic Explosivity Index. This provides the first field-based and ground-truthed estimate of tephra fall volume for a Canadian mafic eruption.

Keywords Small-volume eruptions · Mafic volcanism · Tephra volume · Explosive eruptions · Monogenetic volcanism · Volcanic Explosivity Index

Introduction

Small-scale mafic eruptions occur frequently and produce the most common continental volcanic landforms (Valentine and Gregg 2008). These eruptions can exhibit both effusive and explosive behaviour and often occur in distributed fields (e.g. Valentine and Gregg 2008; Valentine and Connor 2015; Smith and Németh 2017). Hazards include lava flows and tephra fallout, which can affect local communities (e.g. Hill et al. 1998; McDonald et al. 2017; Tsang and Lindsay 2020; Biass et al. 2024) and associated ash plumes that can impact aviation (Tupper et al. 2007; Delbrel et al. 2025). However, planning for future events is difficult without an understanding of past eruptions, especially their erupted volume. Volcanoes in Canada have been little studied due partly to their remote locations, often in mountainous and forested areas, making fieldwork logistically challenging (Russell et al. 2023). Following a preliminary survey of tephra fall from the ~ 1700 CE eruption of *Sii Aks* (Tseax) volcano (pronounced see-ax) in British Columbia (Gallo 2018), we conducted a more comprehensive study to better constrain the tephra volume and deposit. Over several field seasons, we collected thickness data at 96 locations, and here present a quantitative estimate of tephra volume for this eruption, the first such field-based estimate for a Canadian mafic eruption.

Geological setting

The Northern Cordillera Volcanic Province (NCVP) is one of five volcanic regions in western Canada (Fig. 1a, b). It extends ~ 1200 km from northwestern British Columbia to eastern Alaska and has been the source of eruptive activity for > 10 Ma (Edwards and Russell 2000). The NCVP is the most active volcanic province in Canada, with > 100 volcanic centres identified, totalling ~ 1900 km^3 (Edwards and

Editorial responsibility: M. Edmonds

✉ Thomas J. Jones
thomas.jones@lancaster.ac.uk

[1] Lancaster Environment Centre, Lancaster University, Lancaster, UK

[2] Natural Resources Canada, Geological Survey of Canada, Vancouver, BC, Canada

[3] Department of Earth, Ocean and Atmospheric Sciences, University of British Columbia, Vancouver, BC, Canada

[4] Centre for Natural Hazards Research, Department of Earth Sciences, Simon Fraser University, Burnaby, BC, Canada

Published online: 28 January 2026

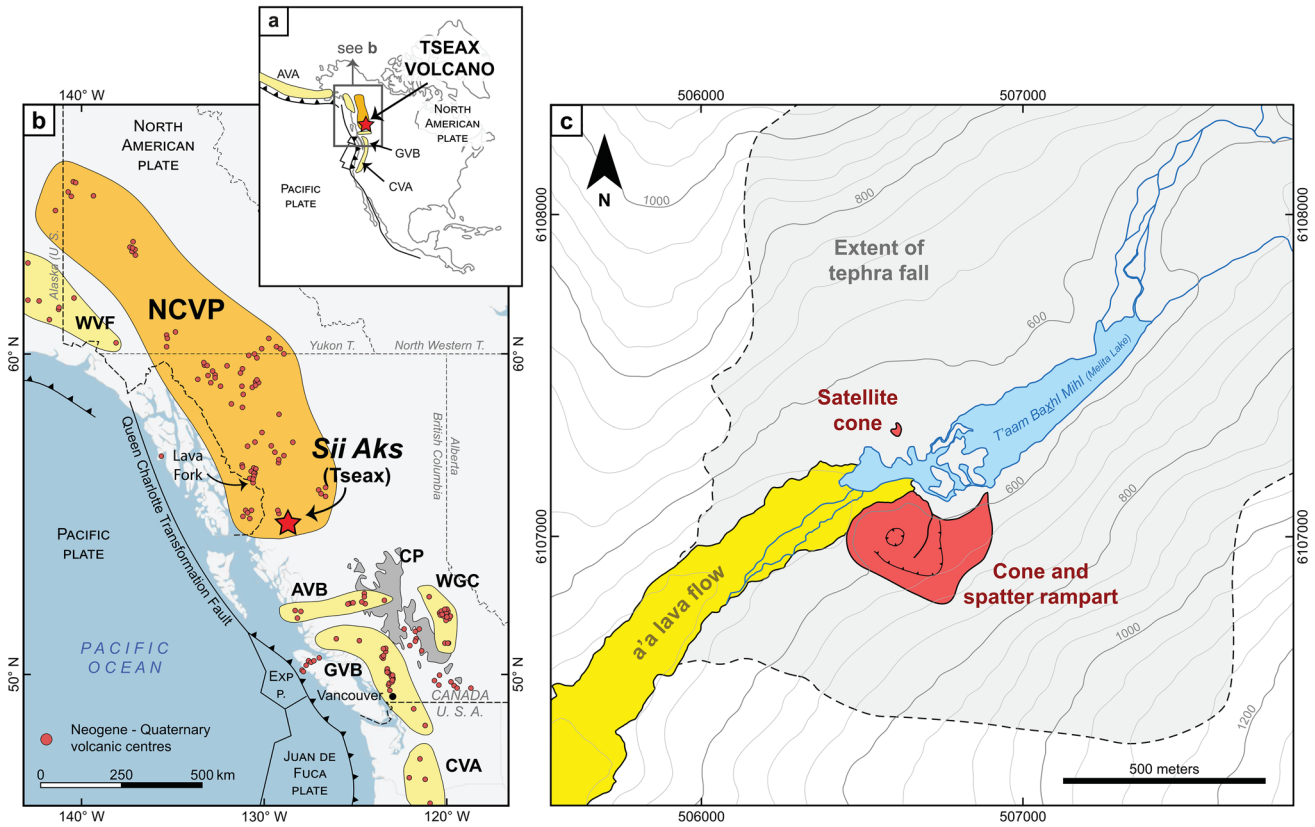

Fig. 1 Location of *Sii Aks* (Tseax) within **a** North America and **b** the volcanic regions of western Canada. AVA, Aleutian Volcanic Arc; AVB, Anaheim Volcanic Belt; CVA, Cascades Volcanic Arc; GVB, Garibaldi Volcanic Belt; NCVP, Northern Cordillera Volcanic Province; WGC, Wells Gray Clearwater Volcanic Field; WVF, Wrangell Volcanic Field. Coordinate system WGS84. **c** *Sii Aks* (Tseax) cone and approximate extent of tephra fallout. Coordinate system UTM 9 N, WGS 84 Datum. Contour interval is 50 m. Figure modified from Le Moigne et al. (2022b)

Russell 2000; Russell et al. 2023). The geochemical signature of the NCVP lavas is consistent with a mantle source having an ocean island basalt-like composition, and volcanism in the NCVP is mainly attributed to upwelling of the asthenosphere related to extensional processes (Edwards and Russell 2000; Batir and Blackwell 2020). The alkaline volcanism may be attributed to adiabatic decompression melting of the lithosphere and a high temperature flux provided by the rise of the underlying asthenosphere to a depth of ~ 65 km (Thorkelson and Taylor 1989; Manthei et al. 2010; Thorkelson et al. 2011; Batir and Blackwell 2020).

The majority of the NCVP volcanoes are small volume edifices (< 1 km^3) that are scattered across British Columbia and Yukon. They consist of isolated pyroclastic cones and associated lava flows and glaciovolcanic edifices (such as tuyas). The majority of lavas are alkali basalts, hawaiites and basanites with subordinate more evolved rocks such as nephelinite and trachyte (Russell et al. 2023). The paucity of radiometric dates and the fact that many centres are partially or entirely glacially eroded makes the spatial and temporal reconstruction of the NCVP difficult. Nevertheless, 37 Holocene eruptions have been identified, suggesting an average recurrence interval of 270 years (Stasiuk et al. 2003). There have been two eruptions in the NCVP within the past 400 years, one at Lava Fork ~ 150 years ago (Elliott et al. 1981) and another at the southernmost volcanic centre *Sii Aks* (Tseax) ~ 1700 CE (Le Moigne et al. 2022b).

The eruption of *Sii Aks* (Tseax) displayed both effusive and explosive behaviour, producing a 32 km-long basanite-trachybasalt lava flow along with a ~ 70 m high scoria cone with spatter rampart and a small (~ 20 m high) satellite cone to the north (Fig. 1c). Trace elements are consistent with melting of a fertile mantle, most likely the upper asthenosphere and a very short residence time in the upper crust before eruption (Le Moigne et al. 2020, 2022a). Oral histories of the Nisga'a First Nation (*Adaawak*) indicate an eighteenth century eruption which lasted days to weeks and occurred during the spawning season for pink salmon in the *Sii Aks* (Tseax) River (between June and September) (Williams-Jones et al. 2020; Le Moigne et al. 2022b; Jones et al. 2025). This is consistent with recent radiocarbon dating which constrains the eruption to 1675–1778 CE (95.4%

probability; Williams-Jones et al. 2020). Lava inundation of three Nisga'a villages resulted in the deaths of up to 2000 people, making this Canada's deadliest volcanic eruption (Le Moigne et al. 2022b).

Methods

Field campaigns

A total of 96 pits were manually dug across the field area (Fig. 1c). The region is densely forested (Fig. 2a) as it is part of the Coastal Western Hemlock biogeoclimatic zone (Pojar et al. 1991), making careful sampling site selection essential to avoid large root disturbance. Where possible, sites were selected on relatively flat ground that showed no evidence of secondary remobilisation (e.g. ground slumping; increasing deposit thicknesses or drainage pathways; reducing deposit thicknesses). Topsoil, moss and roots were removed from each location prior to excavating pits down to the paleosoil horizon at the base of the tephra (Fig. 2b, c). The tephra thicknesses were measured with a metal tape measure, and where the substrate was uneven (e.g. paleo-surface with large blocks), a range in tephra thickness was recorded. The pit location was recorded using a Garmin GPSMAP 64 × handheld GPS (horizontal and vertical accuracy of 3–5 m and 5–10 m, respectively) and subsequently refilled. The small ~ 20 m high satellite cone (Fig. 1c) contained some

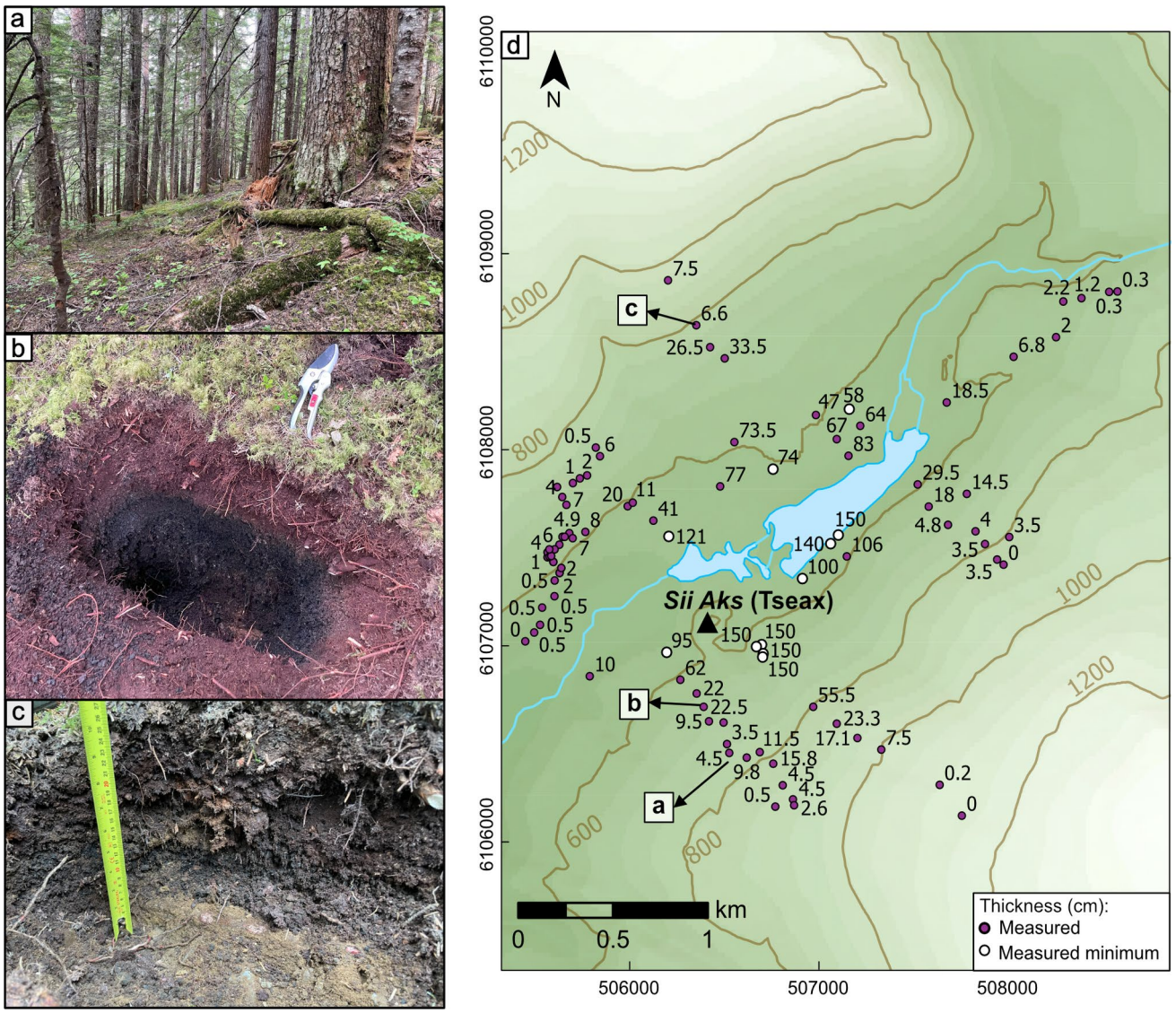

Fig. 2 Observation sites and tephra thicknesses. **a** Fieldwork location in dense forest (trees ~ 30 m tall); **b, c** examples of excavation pits (secateurs/clippers, length ~ 20 cm); **d** map showing measured tephra thicknesses and measurement locations. Coordinate system UTM 9 N, WGS 84 Datum. Contour interval is 200 m

red, oxidised tephra, in contrast to the black tephra from the main *Sii Aks* (Tseax) cone (Jones et al. 2022; Le Moigne et al. 2022b). The red tephra, which suggests high temperatures (e.g. > 700 °C) facilitating iron oxidation (D'Oriano et al. 2013; Moore et al. 2022), only occurred close to the satellite cone and was not mapped as a separate unit. At all locations, the deposit was massive and homogeneous with no layering or grading. Accessory lithics of siltstones, sandstones and mm-size metamorphic and plutonic clasts were observed. These collectively were all very minor and comprise < 1% of the deposit.

Tephra volume calculations

Isopachs (i.e. lines connecting points of equal thickness) were created in ArcGIS Pro using the Empirical Bayesian Kriging geoprocessing tool; this geostatistical interpolation method takes tephra thickness measurements as input and interpolates values between the data points to create best-fit contours. In situations where the pits did not reach the base of the tephra, we used the measured thickness as a minimum value to help constrain the model contours. We used this method to create isopachs from 100 to 10 cm in 10 cm intervals and a 5 cm isopach, and then added a 1 cm isopach by hand as the Kriging interpolation did not produce closed contours for thicknesses < 5 cm. Statistical interpolation reduces the variability inherent in subjective decisions that are made when isopachs are hand-drawn (Klawonn et al. 2014; Engwell et al. 2015). However, we also compared these results with a set of hand-drawn isopachs (described in the Appendix). For our volume calculations (described next), we compared values using the 100 to 5 cm contours and the 100 to 1 cm contours for each method.

The tephra volume (V) was estimated by integrating tephra thickness (T) over the area (A) of the isopachs (Fierstein and Nathenson 1992):

$$V = \int_0^\infty T dA \tag{1}$$

This is typically done by plotting log T vs $\sqrt{A}$, fitting the data to a function and integrating to obtain volume (Pyle 1989, 1995). We compared values obtained from the three most commonly used functions, namely exponential, power law and Weibull and used AshCalc to select the best fit by minimising the mean relative squared error (Daggitt et al. 2014).

In the exponential model, T decays exponentially as $\sqrt{A}$ increases (Eq. 2):

$$T = T_0 \exp^{-k\sqrt{A}} \tag{2}$$

where T_0 is a constant representing the theoretical tephra thickness at the vent and k represents the thinning trend (Pyle 1989; Fierstein and Nathenson 1992). On a semi-log plot of T vs $\sqrt{A}$, the data plot on a straight line with slope -k; multiple straight-line segments can be constructed to account for variable thinning of the deposit.

In the power law model, the relationship between T and $\sqrt{A}$ is described using Eq. 3:

$$T = T_{\mathrm{pl}} \sqrt{A}^{-\mathrm{m}} \tag{3}$$

where T_{pl} is a power-law constant and m represents the thinning trend (Bonadonna et al. 1998; Bonadonna and Houghton 2005). Integration limits must be chosen for this function (since integrating between 0 and ∞ gives the value ∞), and thus, following Bonadonna et al. (1998), we set the proximal limit as the value of $\sqrt{A}$ when $T = T_0$ in Eq. 2. We used $T = 0.1$ cm to select the distal value of $\sqrt{A}$ as no significant amounts of tephra were expected beyond this thickness.

The Weibull model modifies Eq. 2 to take account of variable thinning rates without the need for separate segments:

$$T = \theta \left(\frac{\sqrt{A}}{\lambda}\right)^{n-2} \exp\left(\frac{\sqrt{A}}{\lambda}\right)^{n} \tag{4}$$

where parameters λ, θ, and n are constants which represent the length scale of deposit thinning, a thickness scale, and a shape parameter, respectively (Bonadonna and Costa 2012, 2013).

Results

Tephra thickness

Field locations and measured tephra thicknesses are listed in Table S1 (in the online Supplementary Material 1) and shown in Fig. 2. Sites where the base of the tephra layer was not reached are marked as minimum thicknesses. Tephra thickness was > 150 cm within ~ 200 m of the cone and the deposit extended ~ 3 km to the northeast (downwind).

Isopachs

Isopachs were extrapolated to the northeast where necessary (for thicknesses ≤ 20 cm) to create closed contours. The estimated ground area covered by the deposit (based on an isopach hand-drawn through the three observed points of 0 cm tephra thickness) is 9.4 km^2 (i.e. the outer dashed grey 0 cm line in Fig. 3a). Tephra distribution is constrained to a mountain valley, and the steep topography may enhance deposit reworking in some areas (Fig. 3b, c).

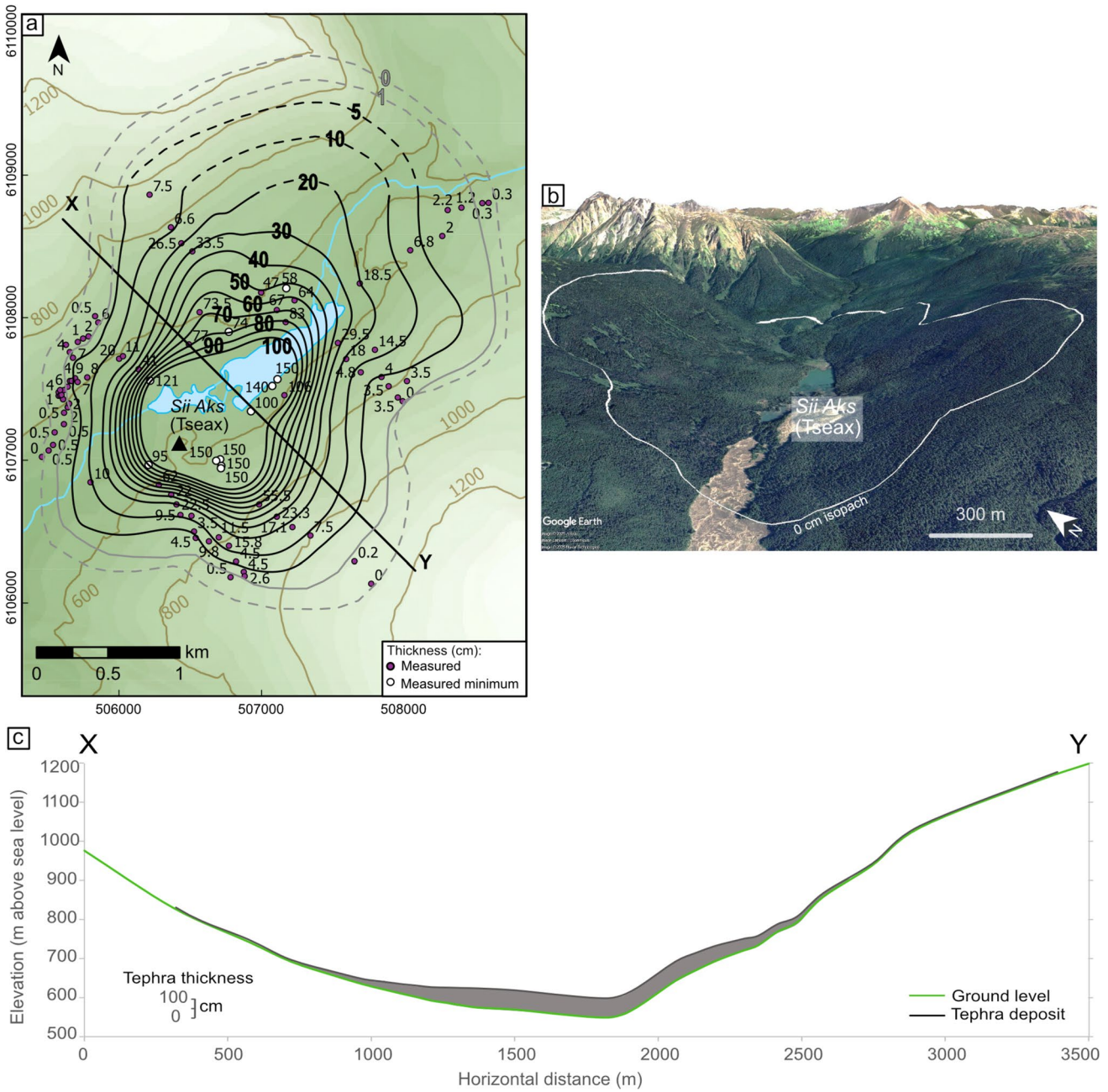

Fig. 3 **a** Measured tephra thicknesses and isopachs. Coordinate system UTM 9N, WGS 84 Datum. Contour interval is 200 m. The large, bold numbers indicate the isopach thickness in cm. The 100 to 5 cm isopachs were created using the ArcGIS Pro Empirical Bayesian Kriging geoprocessing tool. The 1 cm isopach and the estimated extent of the deposit (0 cm isopach) were hand-drawn. Dashed lines indicate extrapolation beyond the field data points. **b** The extent of the tephra deposit (i.e. the 0 cm isopach) shown by the white line overlain on a Google Earth™ image render. **c** The elevation profile and isopach thickness along line XY in Fig. 3a. Note: vertical exaggeration of tephra thickness

Tephra volume and mass

The semilogarithmic relationship between tephra thickness (T) and the square root of isopach area ($\sqrt{A}$) reveals highly consistent trends across multiple models (Fig. 4). The predicted spatial decay of tephra thickness, based on fitting the 100 to 5 cm isopach data, is very similar regardless of the model chosen (i.e. exponential, power-law, or Weibull) (Figs. 4a–d). Similarly, the 100 to 1 cm isopach data, when fitted to the exponential, power-law, and Weibull models, yield comparable results (Figs. 4e–g). Across all models and isopach resolutions, the estimated tephra volumes show strong consistency,

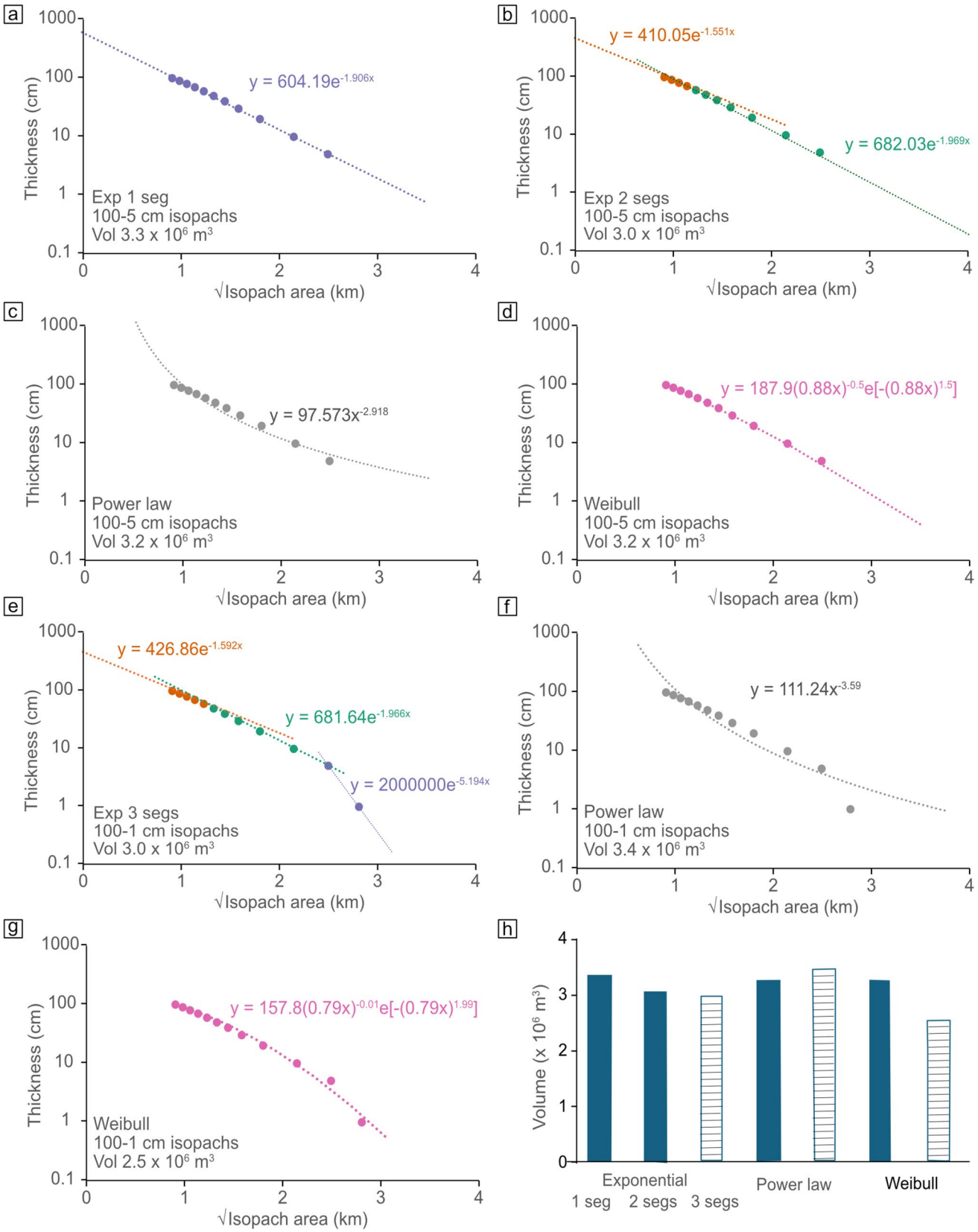
a
y = 604.19e-1.906x
Exp 1 seg
100-5 cm isopachs
Vol 3.3 x 10⁶ m³
b
y = 410.05e-1.551x
y = 682.03e-1.969x
Exp 2 segs
100-5 cm isopachs
Vol 3.0 x 10⁶ m³
c
y = 97.573x-2.918
Power law
100-5 cm isopachs
Vol 3.2 x 10⁶ m³
d
y = 187.9(0.88x)-0.5e[-(0.88x)1.5]
Weibull
100-5 cm isopachs
Vol 3.2 x 10⁶ m³
e
y = 426.86e-1.592x
y = 681.64e-1.966x
y = 2000000e-5.194x
Exp 3 segs
100-1 cm isopachs
Vol 3.0 x 10⁶ m³
f
y = 111.24x-3.59
Power law
100-1 cm isopachs
Vol 3.4 x 10⁶ m³
g
y = 157.8(0.79x)-0.01e[-(0.79x)1.99]
Weibull
100-1 cm isopachs
Vol 2.5 x 10⁶ m³
h
Volume (x 10⁶ m³)
Exponential
1 seg
2 segs
3 segs
Power law
Weibull
Thickness (cm)
√Isopach area (km)

◂**Fig. 4** Tephra thickness vs √isopach area plots used for tephra volume calculations. Tephra thickness vs √isopach area plots for the 100 to 5 cm isopachs using **a** exponential with 1 segment, **b** exponential with 2 segments, **c** power law, and **d** Weibull models, respectively. Tephra thickness vs √isopach area plots for the 100 to 1 cm isopachs using **e** exponential with 3 segments, **f** power law, and **g** Weibull models, respectively. **h** A summary of the volumes obtained from each method. Filled bars indicate that the 100 to 5 cm isopachs were used while hatched bars included the 1 cm isopach

varying only slightly between 2.5 and 3.4×10^6 m^3, indicating a reasonable volume estimate. The volume calculated using the hand-drawn isopachs (100 to 1 cm) and the Weibull model was also consistent at 2.5×10^6 m^3 (detailed in the Appendix).

To estimate the mass of the tephra blanket, we used published data from extensive sampling of the basaltic Tajogaite 2021 deposit on La Palma, Canary Islands. Deposit density ranging from 800 to 1450 kg m^{-3} was reported for samples 1–3 km from the vent (Bonadonna 2022). Using these values, we calculate the mass of the *Sii Aks* (Tseax) tephra blanket as $2.0–4.9\times10^9$ kg.

Discussion and concluding remarks

Creation of isopachs from field data is not a standardised process, and hand-drawn isopachs have been shown to be susceptible to individual bias (Klawonn et al. 2014; Engwell et al. 2015). Using a semi-automated interpolation process in Geographic Information System (GIS) software minimised the bias in producing the isopachs, but the Kriging interpolation method was unable to produce closed contours below 5 cm tephra thickness. To account for tephra volume beyond this contour, we added a hand-drawn 1 cm isopach to better constrain the volume estimates. The results were nevertheless very consistent across all integration models (exponential, power law, and Weibull) both with and without inclusion of the 1 cm isopach. As the isopachs were created using some minimum thickness measurements, the resulting volumes represent minimum values. This is typically the case for all volume estimates based on isopach data, as without industrial excavation machinery, it is rarely possible to dig to the base of the tephra close to a scoria cone. In particular, the estimated tephra volume within the 100 cm isopach does not account for the measured thicknesses of 150 cm where the base of the tephra layer was not reached. This could add ~ 15–20% to the total volume if the tephra deposit within this isopach was in fact 150 cm thick throughout.

Explosive vs effusive eruption volume and VEI classification

The tephra thickness data give an estimated volume of the tephra blanket of $2.5–3.4\times10^6$ m^3. This is relatively small compared to monogenetic basaltic tephra fall volumes at other locations such as Marcath, Nevada (~2×10^7 m^3; Valentine et al. 2017); Blue Lake Crater, Oregon (~4×10^7 m^3; Johnson and Cashman 2020); and Lathrop Wells, Nevada (~7×10^7 m^3; Valentine et al. 2007). In the Auckland Volcanic Field, tephra deposits are not well preserved, but similar tephra blanket volumes of 4.1×10^6 – 4.7×10^7 m^3 have been estimated for three eruptions which occurred within the past 11 ka (Purchas Hill, Mt. Wellington, and Rangitoto; Kereszturi et al. 2013). Previous work at *Sii Aks* (Tseax) estimated the volume of the scoria cone at ~$2.8\pm0.4\times10^6$ m^3, that of the spatter ramparts as ~$1.1\pm0.3\times10^6$ m^3 and the small satellite cone at ~2×10^4 m^3 (Le Moigne et al. 2020). Taken together, the volume of the explosive products is $5.7–8.0\times10^6$ m^3, indicating that this eruption was VEI 2 (i.e. volume of $1–10\times10^6$ m^3; Newhall and Self 1982). The explosive products (tephra blanket and cone) thus only represent ~ 1% of the volume of the lava flow field (0.49 ± 0.08 km^3; Le Moigne et al. 2020) produced during the *Sii Aks* (Tseax) eruption.

Potential hazard

~~Our knowledge of past explosive events in the NCVP is limited, and pyroclastic deposits are generally less well preserved than lavas. The recent eruptions at *Sii Aks* (Tseax) and Lava Fork (< 400 years) show that the region is still volcanically active. The volcanic edifices and deposits are well preserved and provide a means to constrain the behaviour and magnitude of such small volume events. These insights support hazard evaluation scenarios. Small mafic eruptions are the most frequent form of subaerial volcanism, and thus, our analysis of the explosive phase of the ~ 1700 CE eruption of *Sii Aks* (Tseax) serves as a template for interpreting older mafic volcanic successions across the NCVP. The area affected by tephra fallout during any future eruption will depend on the meteorological conditions (i.e. wind direction, wind speed, precipitation) at the time of the event. Furthermore, as most NCVP volcanoes are located within mountainous areas, topography might influence the post-depositional distribution of the deposit. The population of northwestern Canada is low, and hence, any impacts on settlements are likely to be localised. However, the tephra loadings in this study are sufficient to cause road disruption (> 0.1–1 mm; Blake et al. 2017) and building damage (> 10 cm; Jenkins et al. 2015). Ash plumes from explosive eruptions could also affect air traffic over western Canada, although the risk is minimal for mafic lava fountains such as *Sii Aks* (Tseax).~~

Appendix Comparison of hand- drawn isopachs with those created by ArcGIS kriging

We asked 13 volcanologists to hand-draw isopachs based on the tephra thickness measurements used for the ArcGIS Pro Empirical Bayesian Kriging. They drew 100–10 cm isopachs

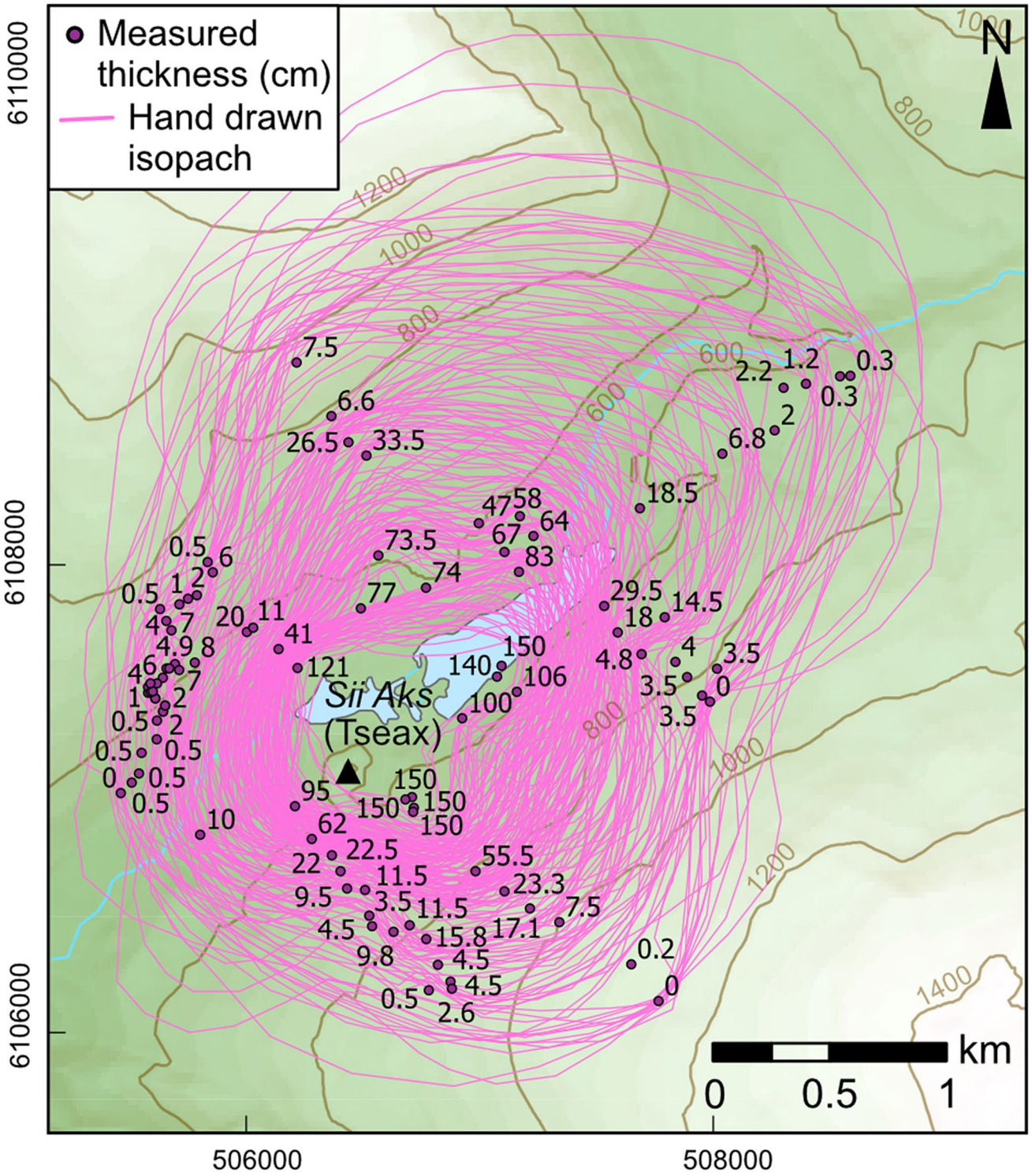

Fig. 5 Measured tephra thicknesses and isopachs drawn by hand by 13 volcanologists. Coordinate system UTM 9 N, WGS 84 Datum. Contour interval is 200 m

in 10 cm intervals, plus 5 cm, 1 cm and 0 cm isopachs, to allow comparison with our results from kriging supplemented by hand drawing (see "Tephra volume calculations" section). The hand-drawn isopachs are shown in Supplementary Material 2, Fig. S1 and summarised in Fig. 5. We took the median area for each 100–1 cm isopach (Table S2) and used the Weibull method (Bonadonna and Costa 2012, 2013) to calculate tephra volume (Fig. 6). The calculated tephra

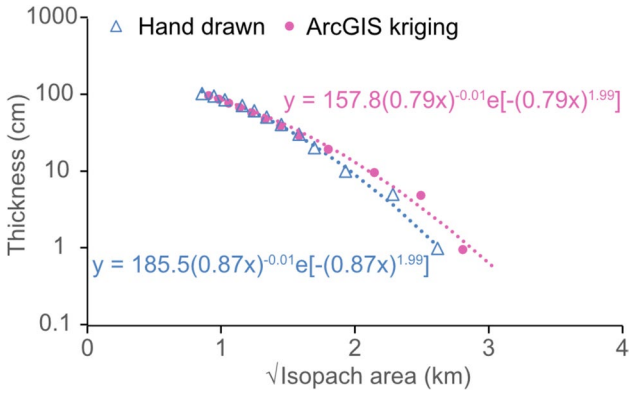

Fig. 6 Tephra thickness vs √isopach area plot used for tephra volume calculations with the Weibull model, for 100–1 cm isopachs drawn by hand and created using the ArcGIS Pro Empirical Bayesian Kriging geoprocessing tool

volume from the hand-drawn contours is 2.5×10^6 m^3, the same as the value obtained with the Weibull function using isopachs from ArcGIS kriging (Fig. 4).

Supplementary Information The online version contains supplementary material available at https://doi.org/10.1007/s00445-026-01941-5.

Acknowledgements The authors thank Dr. Deana Nyce and Harry Nyce Jr. of the Wilp Wilx̱o'oskwhl Nisga'a Institute (WWNI) for their continued and enthusiastic support. This research was carried out as part of B.C. Parks/NLG permits 108312 and 111814.

Author contribution TJJ designed the study, supervised the project, and acquired the funding. TJJ, KMcC, YLM, JKR, and GWJ conducted the fieldwork. SO was responsible for all formal data analysis and produced the original draft manuscript. All authors reviewed and edited the submitted manuscript.

Funding The authors of this work were supported by a UK Research and Innovation (UKRI) Future Leaders Fellowship (MR/W009781/1) awarded to TJJ.

Data availability All data are included in Supplementary material.

Code availability Not applicable.

Declarations

Conflict of interest The authors declare no competing interests.

References

Batir JF, Blackwell DD (2020) Thermal evolution of the Northern Cordillera Volcanic Province: implication for heat flow in remnant back-arc regions. Int Geol Rev 62:1510–1537. https://doi.org/10.1080/00206814.2019.1658230

Biass S, Reyes-Hardy M-P, Gregg C et al (2024) The spatiotemporal evolution of compound impacts from lava flow and tephra fallout on buildings: lessons from the 2021 Tajogaite eruption (La Palma, Spain). Bull Volcanol 86:10. https://doi.org/10.1007/s00445-023-01700-w

Blake DM, Deligne NI, Wilson TM et al (2017) Improving volcanic ash fragility functions through laboratory studies: example of surface transportation networks. J Appl Volcanol 6:16. https://doi.org/10.1186/s13617-017-0066-5

Bonadonna C, Costa A (2012) Estimating the volume of tephra deposits: a new simple strategy. Geology 40:415–418. https://doi.org/10.1130/G32769.1

Bonadonna C, Costa A (2013) Plume height, volume, and classification of explosive volcanic eruptions based on the Weibull function. Bull Volcanol 75:742. https://doi.org/10.1007/s00445-013-0742-1

Bonadonna C, Houghton BF (2005) Total grain-size distribution and volume of tephra-fall deposits. Bull Volcanol 67:441–456. https://doi.org/10.1007/s00445-004-0386-2

Bonadonna C, Ernst GGJ, Sparks RSJ (1998) Thickness variations and volume estimates of tephra fall deposits: the importance of particle Reynolds number. J Volcanol Geotherm Res 81:173–187. https://doi.org/10.1016/S0377-0273(98)00007-9

D'Oriano C, Pompilio M, Bertagnini A et al (2013) Effects of experimental reheating of natural basaltic ash at different temperatures and redox conditions. Contrib Mineral Petrol 165:863–883. https://doi.org/10.1007/s00410-012-0839-0

Daggitt ML, Mather TA, Pyle DM, Page S (2014) AshCalc–a new tool for the comparison of the exponential, power-law and Weibull models of tephra deposition. J Appl Volcanol 3:7. https://doi.org/10.1186/2191-5040-3-7

Delbrel J, Burton M, Engwell S et al (2025) An investigation of changes to commercial aircraft flight paths during volcanic eruptions. J Appl Volcanol 14:2. https://doi.org/10.1186/s13617-025-00150-7

Edwards BR, Russell JK (2000) Distribution, nature, and origin of Neogene-Quaternary magmatism in the northern Cordilleran volcanic province, Canada. Geol Soc Am Bull 112(8):1280–1295

Elliott RL, Koch RD, Robinson SW (1981) Age of basalt flows in the Blue River Valley, Bradfield Canal Quadrangle. The United States Geological Survey in Alaska: accomplishments during 1979. US Geol Surv Circ 0823-B:115–116

Engwell SL, Aspinall WP, Sparks RSJ (2015) An objective method for the production of isopach maps and implications for the estimation of tephra deposit volumes and their uncertainties. Bull Volcanol 77:61. https://doi.org/10.1007/s00445-015-0942-y

Fierstein J, Nathenson M (1992) Another look at the calculation of fallout tephra volumes. Bull Volcanol 54:156–167. https://doi.org/10.1007/BF00278005

Gallo R (2018) History and dynamics of explosive volcanism at Tseax Cone, British Columbia. https://open.library.ubc.ca/collections/undergraduateresearch/52966/items/1.0366164. Accessed 8 Aug 2025

Hill BE, Connor CB, Jarzemba MS et al (1998) 1995 eruptions of Cerro Negro volcano, Nicaragua, and risk assessment for future eruptions. Geol Soc Am Bull 110(10):1231–1241

Jenkins SF, Wilson T, Magill C et al (2015) Volcanic ash fall hazard and risk. In: Loughlin SC, Sparks RSJ, Brown SK et al (eds) Global volcanic hazards and risk. Cambridge University Press, Cambridge, pp 173–221

Johnson ER, Cashman KV (2020) Understanding the storage conditions and fluctuating eruption style of a young monogenetic volcano: Blue Lake crater (<3 ka), High Cascades, Oregon. J Volcanol Geotherm Res 408:107103. https://doi.org/10.1016/j.jvolgeores.2020.107103

Jones TJ, Le Moigne Y, Russell JK et al (2022) Inflated pyroclasts in proximal fallout deposits reveal abrupt transitions in eruption behaviour. Nat Commun 13:2832. https://doi.org/10.1038/s41467-022-30501-6

Jones TJ, Williams-Jones G, Nyce H (2025) Braiding indigenous knowledge systems and Western science through co-creation and co-teaching. Front Earth Sci 13:1587092. https://doi.org/10.3389/feart.2025.1587092

Kereszturi G, Németh K, Cronin SJ et al (2013) A model for calculating eruptive volumes for monogenetic volcanoes — implication for the Quaternary Auckland Volcanic Field, New Zealand. J Volcanol Geotherm Res 266:16–33. https://doi.org/10.1016/J.JVOLGEORES.2013.09.003

Klawonn M, Houghton BF, Swanson DA et al (2014) From field data to volumes: constraining uncertainties in pyroclastic eruption parameters. Bull Volcanol 76:839. https://doi.org/10.1007/s00445-014-0839-1

Le Moigne Y, Williams-Jones G, Russell K, Quane S (2020) Physical volcanology of Tseax Volcano, British Columbia, Canada. J Maps 16:363–375. https://doi.org/10.1080/17445647.2020.1758809

Le Moigne Y, Vigouroux N, Russell JK, Williams-Jones G (2022a) Magmatic origins and storage conditions for the historic eruption of Tseax Volcano, British Columbia, Canada. Chem Geol 588:120648. https://doi.org/10.1016/j.chemgeo.2021.120648

Le Moigne Y, Williams-Jones G, Vigouroux N, Russell JK (2022b) Chronology and eruption dynamics of the historic~1700 CE eruption of Tseax Volcano, British Columbia, Canada. Front Earth Sci. https://doi.org/10.3389/feart.2022.910451

Manthei CD, Ducea MN, Girardi JD et al (2010) Isotopic and geochemical evidence for a recent transition in mantle chemistry beneath the western Canadian Cordillera. J Geophys Res Solid Earth. https://doi.org/10.1029/2009JB006562

McDonald GW, Smith NJ, Kim J et al (2017) The spatial and temporal 'cost' of volcanic eruptions: assessing economic impact, business inoperability, and spatial distribution of risk in the Auckland region, New Zealand. Bull Volcanol 79:48. https://doi.org/10.1007/s00445-017-1133-9

Moore HC, Carey RJ, Houghton BF et al (2022) High-temperature oxidation of proximal basaltic pyroclasts, 1886 Tarawera, New Zealand. Bull Volcanol 84:46. https://doi.org/10.1007/s00445-022-01549-5

Newhall CG, Self S (1982) The volcanic explosivity index (VEI) an estimate of explosive magnitude for historical volcanism. J Geophys Res 87:1231. https://doi.org/10.1029/JC087iC02p01231

Pojar J, Klinka K, Demarchi DA (1991) Coastal western hemlock zone. In: Meidinger D, Pojar J (eds) Ecosystems of British Columbia. Ministry of Forests, Victoria, B.C., pp 95–111

Pyle DM (1989) The thickness, volume and grainsize of tephra fall deposits. Bull Volcanol 51:1–15. https://doi.org/10.1007/BF01086757

Pyle DM (1995) Assessment of the minimum volume of tephra fall deposits. J Volcanol Geotherm Res 69:379–382. https://doi.org/10.1016/0377-0273(95)00038-0

Russell JK, Edwards BR, Williams-Jones G, Hickson CJ (2023) Pleistocene to Holocene volcanism in the Canadian Cordillera. Can J Earth Sci 60:1443–1466. https://doi.org/10.1139/cjes-2023-0065

Smith IEM, Németh K (2017) Source to surface model of monogenetic volcanism: a critical review. Geol Soc London Spec Publ 446:1–28. https://doi.org/10.1144/SP446.14

Stasiuk M, Hickson C, Mulder T (2003) The vulnerability of Canada to volcanic hazards. Nat Hazards 28:563–589. https://doi.org/10.1023/A:1022954829974

Thorkelson DJ, Taylor RP (1989) Cordilleran slab windows. Geology 17:833–836. https://doi.org/10.1130/0091-7613(1989)0170833:CSW2.3.CO;2

Thorkelson DJ, Madsen JK, Sluggett CL (2011) Mantle flow through the Northern Cordilleran slab window revealed by volcanic geochemistry. Geology 39:267–270. https://doi.org/10.1130/G31522.1

Tsang SWR, Lindsay JM (2020) Lava flow crises in inhabited areas part I: lessons learned and research gaps related to effusive, basaltic eruptions. J Appl Volcanol 9:9. https://doi.org/10.1186/s13617-020-00096-y

Tupper A, Guffanti M, Rose B et al (2007) The "Gulfstream incident": twin-engined flame-out over the Papua New Guinea highlands. In: 4th International Workshop on Volcanic Ash, Rotorua, New Zealand, 26–30 Mar 2007 [Proceedings]. World Meteorological Organization. https://aviationtraining.wmo.int/pluginfile.php/44/mod_resource/content/0/VWS/20_VAWS4WP0703_1_.pdf. Accessed 30 July 2025

Valentine GA, Connor CB (2015) Basaltic volcanic fields. In: Sigurdsson H, Houghton BF, McNutt SR, Rymer H (eds) Encyclopedia of Volcanoes, 2nd edn. Elsevier, Oxford, pp 423–439

Valentine GA, Gregg TKP (2008) Continental basaltic volcanoes — processes and problems. J Volcanol Geotherm Res 177:857–873. https://doi.org/10.1016/j.jvolgeores.2008.01.050

Valentine GA, Krier DJ, Perry FV, Heiken G (2007) Eruptive and geomorphic processes at the Lathrop Wells scoria cone volcano. J Volcanol Geotherm Res 161:57–80. https://doi.org/10.1016/j.jvolgeores.2006.11.003

Valentine GA, Cortés JA, Widom E et al (2017) Lunar crater volcanic field (Reveille and Pancake Ranges, Basin and Range Province, Nevada, USA). Geosphere 13:391–438. https://doi.org/10.1130/GES01428.1

Williams-Jones G, Barendregt RW, Russell JK et al (2020) The age of the Tseax volcanic eruption, British Columbia, Canada. Can J Earth Sci 57:1238–1253. https://doi.org/10.1139/cjes-2019-0240